

Journal of
**Micro/Nanolithography,
MEMS, and MOEMS**

SPIEDigitalLibrary.org/jm3

**Scanning acoustic gigahertz
microscopy for metrology
applications in three-dimensional
integration technologies**

Sebastian Brand
Adriana Lapadatu
Tatjana Djuric
Peter Czurratis
Jan Schischka
Matthias Petzold



SPIE

Scanning acoustic gigahertz microscopy for metrology applications in three-dimensional integration technologies

Sebastian Brand,^{a,*} Adriana Lapadatu,^c Tatjana Djuric,^b Peter Czurratis,^b Jan Schischka,^a and Matthias Petzold^a

^aFraunhofer Institute for Mechanics of Materials IWM, Center for Applied Microstructure Diagnostics CAM, 06120 Halle, Germany

^bPVA TePla Analytical Systems GmbH, 73463 Westhausen, Germany

^cSensoror, 3194 Horten, Norway

Abstract. Current trends in microelectronics focus on three-dimensionally integrating different components to allow for increasing density and functionality of integrated systems. Concepts pursued involve vertical stacking and interconnecting technologies that employ micro bumping, wafer bonding, and through silicon vias (TSVs). Both the increasing complexity and the miniaturization of key elements in three-dimensional (3-D) components lead to new requirements on inspection and metrology tools and techniques as well as for failure analysis methodologies. For metrology and quality assessment in particular, methods operating nondestructively are of major importance. Scanning acoustic microscopy has the ability of illuminating optically opaque materials and, thus, allowing the assessment and imaging of internal structures. Conventional scanning acoustic microscopy (SAM) equipment can be applied to analyze the quality of wafer-bonded interfaces in 3-D integration but may reach its limitations when structures shrink in size and gain complexity. A new concept of acoustic inspection in the gigahertz (GHz) frequency band is explored for its applicability to 3-D integration technologies. Extending the acoustic inspection frequency allows for lateral resolutions in the 1- μ m range and also enables the inspection of microbumps and TSVs in addition to wafer bonded interfaces, which exceed the applicability of conventional SAM. Three case studies are presented here ranging from conventional SAM on a full wafer scale to acoustic GHz microscopy on thin films and TSVs. © The Authors. Published by SPIE under a Creative Commons Attribution 3.0 Unported License. Distribution or reproduction of this work in whole or in part requires full attribution of the original publication, including its DOI. [DOI: [10.1117/1.JMM.13.1.011207](https://doi.org/10.1117/1.JMM.13.1.011207)]

Keywords: three-dimensional integration; scanning acoustic microscopy; gigahertz scanning acoustic microscopy; acoustic gigahertz microscopy; nondestructive through silicon via inspection.

Paper 13151SS received Aug. 23, 2013; revised manuscript received Jan. 8, 2014; accepted for publication Jan. 15, 2014; published online Feb. 20, 2014.

1 Introduction

Over the last years, technologies enabling three-dimensional (3-D) integration of semiconductor devices have rapidly attracted attention. The driving forces behind these developments result from the same requirements that have been pushing microelectronics for decades—to optimize performance in terms of data speed and to reduce transmission losses, to increase miniaturization, and to integrate more functionality in smaller and smaller volumes while maintaining reliability, time-to-market, and cost efficiency. Today, many experts see a bright future for 3-D integration although there are currently still some questions to be addressed. These are, on one hand, related to the appropriate business models and the application fields in which the technical benefits of 3-D integration will outbalance the increased manufacturing costs. On the other hand, further developments are also required regarding the 3-D integration manufacturing ecosystem with respect to quality control and reliability issues.

Technically, 3-D integration involves a variety of key processing steps, such as improved wafer thinning and handling, formation of through silicon vias (TSVs), vertical chip stacking or wafer bonding of different types of semiconductors, and generation of electrical chip-to-chip interconnections in the bonding interface together with signal

redistribution systems. TSVs are typically formed by reactive ion etching followed by complex processes of via isolation (liner formation), seed layer deposition, via filling, and, as the last step in many cases, Cu electroplating. Vertical chip bonding and interconnection can be accomplished by using intermediate polymer films for attachment and microbumps for electrical contact formation. Wafer bonding approaches, including Si direct bonding, thermocompression bonding, or hybrid bonding combining both oxide and metal bonding, provide alternative process approaches. In terms of the process flow, different concepts have been proposed utilizing either TSV first, TSV middle, or TSV last technologies depending on whether the TSV formation is performed before or after the semiconductor front end processes and the bonding steps.

On the other hand, the complexity of 3-D high-density integration with respect to novel designs, processes, and materials leads to new challenges for metrology, quality assurance, and failure analysis that have to be met prior to mass manufacturing. For example, the reduced access for inspection and microstructure diagnostics in vertically stacked components compared to standard ICs or MEMS components is a major issue. In particular, the variety of electrically functional routings (TSV, electrical redistribution systems) and interconnects that are now buried within the chip or in chip-to-chip interfaces pose severe challenges to the testing and defect characterization methods. As a consequence, new and adequately adapted techniques and tools applicable for metrology of the key process steps in

*Address all correspondence to: Sebastian Brand, E-mail: Sebastian.Brand@iwmh.fraunhofer.de

3-D integration as well as for failure analysis have to be developed. For these purposes, nondestructive analysis methods are preferred if applicable. Since scanning acoustic microscopy (SAM) is an already well-established methodology for defect analysis of wafer-bonded interfaces of MEMS components, it is rather straightforward to also consider SAM techniques as inspection tools for 3-D integration.

In this paper, novel methodical SAM approaches for defect characterization in 3-D integrated components are shown exemplarily. The potential of these techniques is illustrated for a 3-D-integrated sensor component formed by Si direct bonding with a TSV last process, focusing on the quality of the bonding steps. The challenge is to detect small bonding voids in the interfaces while the thickness of the wafers can range between $\sim 800 \mu\text{m}$ (before thinning) and $< 50 \mu\text{m}$ (after thinning). In addition, the localization of non-contacting interconnects (electrical opens) and also of voids in the polymeric intermediate layers within the chip-to-chip interfaces of 3-D integrated components is of major importance. A potential approach addressed in this paper consists of expanding the application of acoustic microscopy to the gigahertz (GHz) frequency range, enabling much higher spatial resolutions. Case studies will be presented demonstrating the benefit of GHz SAM analysis to defect analysis for both thin films and Cu-filled TSV. It will be shown that advanced SAM analysis techniques can significantly contribute to secured and improved quality and reliability properties of complex 3-D devices and systems.

2 Scanning Acoustic Microscopy

2.1 Conventional SAM

In many fields—especially in failure analysis, quality assessment, or process development—the availability of test and inspection methods that operate nondestructively is of major importance. The benefit of those measurement techniques ranges from the assessment of an overview of a specimen's condition to detailed high-resolution defect detection, localization, and evaluation. Although a variety of non-destructive imaging and validation techniques exist, the contrast mechanisms on which the visualization is based vary drastically between the individual methods. While in x-ray inspection the absorption of electromagnetic waves in the x-ray band is employed for imaging, thermographic inspection methods are based on the emission and detection of electromagnetic waves in the infrared band. SAM, which is been focused on in this study, employs elastic waves that mechanically interact with the materials/structures encountered during propagation. The contrast mechanism of methods that use mechanical waves is based on the reflection, transmission, or scattering of an insonated pressure wave. The interaction of acoustical waves is extremely sensitive to the elastic properties and the mass density of the specimen under investigation and the angle of incidence. While reflection occurs on interfaces between materials with differing acoustic impedances, which have a lateral dimension above the wavelength of the acoustical wave, sound waves will be scattered when encountering impedance mismatches with effective size fractions below the wavelength. In SAM, attention is often only paid to the reflected compressional component of the insonated acoustic wave. However, material-specific characteristic phenomena will occur when

an acoustic wave interacts with an interface under an angle other than 90 deg, resulting in the excitation of additional wave modes with various polarizations.

The main application of SAM uses focused sound waves in the ultrasonic frequency band, commonly in the range between 5 and 200 MHz. Upon a trigger signal, a spike pulse is produced that excites a piezo element, which is contained in an ultrasonic transducer, to a broadband oscillation. The bandwidth of that oscillation depends on the mechanical and structural specifics of the transducer element. It is commonly desired to excite short pulses since that allows for an increased axial resolution. The number of oscillations and the frequency of the excited wave define the pulse length and, thus, limit the axial resolution. However, since acoustic microscopes are intended and capable of covering a broad frequency range, the actual inspection frequency and the pulse specifics can be adjusted upon selecting a most appropriate transducer for a specific inspection task. As may become clear from the descriptions above, acoustic waves can be focused just like other wave types. However, since the sound velocity in a solid usually exceeds the values in gases or fluids, acoustic lenses are commonly concave in order to provide the radially decreasing phase shift required for focusing. In case of an acoustic lens, the numerical aperture, which includes the radius of curvature and the opening angle, defines the achievable lateral resolution. However, due to the difference in sound velocity between the coupling medium and a solid sample, the theoretical value of the lateral resolution deviates from the actual achievable value inside the solid. A short pulse of focused sound waves is then transmitted from the acoustic lens into the coupling medium and further into the sample, where it undergoes reflection and scattering that send parts of the insonated waves back into the direction of the transducer. In acoustic inspection in pulse-echo mode, the same focusing ultrasonic transducer that transmits the acoustic pulse is also used for receiving echoes occurring at boundaries between materials/structures of differing acoustic impedance values. The reflectivity of those interfaces is defined by the acoustic impedance mismatch resulting from the differences in mass density and sound velocity, representing the material's elastic properties. In case of delamination, the resulting reflectivity is close to one, caused by the immense difference in mass density and elastic properties between the solid sample and the gaseous layer originating the delamination. This fact enables acoustic microscopy to detect delamination defects even with lateral dimensions much below the actual resolution, hence requiring the discrimination between detection and resolution limit.

With its capability to nondestructively illuminate optically opaque materials and to enable high-resolution imaging, SAM is a unique and powerful tool for the application in failure analysis, quality assessment, and nondestructive testing.

Conventional acoustic microscopy tools operate in the frequency band up to 200 MHz allowing for theoretical resolutions of 15 to 20 μm depending on the focusing behavior of the ultrasonic transducer employed. The selection of an appropriate lens is essential for successfully solving the required inspection task. The higher the focusing of an acoustic lens, the higher the achievable lateral resolution, but the lower the depth of field defining that axial range where signal acquisition is possible.

When sample structures get smaller in both axial and lateral directions, it becomes increasingly challenging to reliably inspect and analyze the echo signals received. As wafers get thinner, the echo signal occurring at the top surface and the bond interface start to interfere, which can be compensated for up to a certain extent. However, when it comes to thin films or wafer thicknesses $<80 \mu\text{m}$, a differentiation between those signals can no longer be made, consequently requiring an adaptation of the inspection method by drastically increasing the acoustic frequency and/or the numerical aperture resulting in a higher lateral and axial resolution.

2.2 Scanning GHz Acoustic Microscopy

Recent developments in the field of SAM have been focused on inspection and metrology of decreasing structure dimensions, which are of major relevance for the emerging technologies aiming at the 3-D integration in the semiconductor industry and the field of microelectronics, thus providing applicable equipment with the benefits of acoustic inspection. The main challenges in this field of research and development have been the increase in the acoustic frequency of up to 2 GHz and the manufacturing of numerical apertures of acoustic lenses for enabling inspection resolutions of $<1 \mu\text{m}$.^{1,2} By increasing the acoustic frequency, the fact of wave-attenuation and the excitation of additional wave modes can no longer remain neglected. Since acoustic attenuation increases exponentially with frequency, the pulse energy and, thus, the length of the transmitted pulse had to be increased, resulting in a decreased fractional bandwidth at a much higher frequency. By outfitting the acoustic GHz microscope with lenses whose apertures have focusing numbers <1 , the opening angle is ~ 100 deg. The consequence of this adjustment is the insonation at large angles, resulting in additional wave modes excited at and in the sample surface³ and a drastic decrease in the depth of field of the acoustic diffraction pattern of the lens, allowing an increased axial resolution even though the fractional bandwidth decreased and, thus, resulting in an increase of the relative pulse length. While at the first glimpse those facts might appear disadvantageous, they actually allow overcoming the main challenges arising for acoustic inspection at the extreme frequencies in the GHz band. Acoustic GHz microscopy offers both conventional-like imaging at resolutions in the $1\text{-}\mu\text{m}$ scale and also allows the employment of additional modes that can, for example, only propagate in the sample surface or modes that propagate as lamb waves in a film with thickness of $\sim 1 \mu\text{m}$ and below. It, thus, not only extends the imaging resolution, but also provides access to actual physical properties of the sample in a nondestructively operating manner at a $1\text{-}\mu\text{m}$ scale.

2.3 GHz SAM Equipment and Analysis

The results of two case studies that used acoustic GHz microscopy for high-resolution acoustical imaging at 1 GHz are being presented here. The aim of those studies was the nondestructive localization of defects and irregularities buried closely beneath the sample surface. While the first example aimed at evaluating defect-related irregularities in the bond interface, the second study was geared at detecting voids inside TSVs.

The setup employed in the current work was a GHz SAM (PVA TePla Analytical Systems GmbH, Westhausen, Germany) that was developed in close collaboration between PVA TePla Analytical Systems and the Fraunhofer IWM-Halle. The microscope was equipped with a 1-GHz acoustical lens (opening angle: 100 deg; focal length $80 \mu\text{m}$ in water). Figure 1 contains a photograph and a schematic of the working principle of the GHz SAM. The scan range of this microscope can be defined freely between $50 \mu\text{m}$ and 2 mm, while the line repetition frequency can be adjusted between 10 and 50 Hz, allowing fast acquisition of the GHz micrographs. The acoustic frequency of the microscope was set to 1.12 GHz. The length of the transmit pulse, which can also be varied in steps of 10 ns, providing another degree of freedom, was set to 30 ns for inspecting the examples shown here. To ensure spatial oversampling and to increase the signal-to-noise ratio (SNR), pulses were transmitted at a repetition rate of 400 kHz. Received echo signals have been amplified, gated, and preprocessed inside the microscope. Besides unprocessed raw data, the GHz microscope provides the peak detected and enveloped line signal, which represents the acoustic energy along a scan line. The advantage of this internal preprocessing of the received rf signals is a largely increased SNR that allows for rapid high-resolution acoustical imaging. Data shown here were recorded in V(z) mode, meaning that at least 25 scan planes were acquired at $1\text{-}\mu\text{m}$ increments for decreasing distances between sample and acoustic lens, resulting in a defocus of at least $20 \mu\text{m}$. Defocusing the large numerical aperture of the acoustical lens allows for placing its focus beneath the surface of the sample and also results in the excitation of surface acoustic waves due to an increased angle of insonation. During data acquisition, a droplet of deionized and degassed water at 21°C was used as couplant for matching acoustic impedances and to increase sound wave transmission. It was not necessary to submerge the entire sample in water during the acoustic scans, thus avoiding potential harm that may occur to the sample by fluid exposition.

3 Case Studies

3.1 Conventional SAM on Bonded Wafer Pair Containing TSV Structures Supplemented by Signal Analysis for Optimizing Imaging Contrast and Resolution

The results presented here include a case study employing acoustic microscopy on samples representing an innovative 3-D sensor integration concept.⁴ In this approach, an application-optimized sensor layer is processed on a specific wafer substrate. The sensor is vertically connected to a readout circuitry chip produced in standard CMOS technology by Si direct wafer bonding. Electrical interconnects are formed using a quality-proven “open” via last TSV technology. The substrate wafer is prepared by plasma enhanced chemical vapor deposition (PECVD) oxide deposition, densification, chemical-mechanical polishing followed by an optimized planarization process and wet chemistry cleaning. Bonding is done using a low-temperature nitrogen plasma activated fusion bond process with additional annealing. The potential formation of bonding voids has to be controlled in order to secure the quality of the bonding process. With respect to 3-D integration using a via-last process,

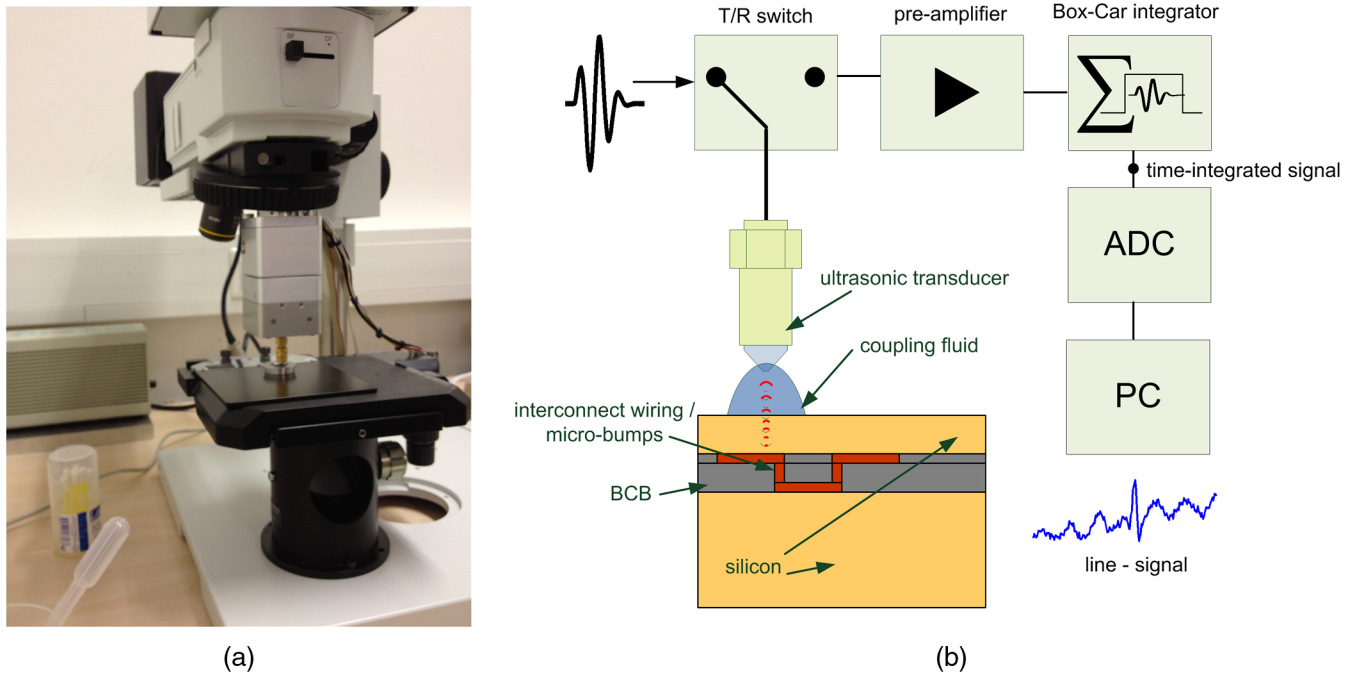


Fig. 1 Gigahertz (GHz) scanning acoustic microscopy (SAM) employed for high-resolution acoustical imaging at 1 GHz for inspecting microbumps and through silicon vias (TSVs). (a) photograph of the scanner unit including a 1-GHz acoustical lens. (b) schematics of the GHz-SAM for generation, transmission, and reception of 1-GHz acoustic signals, including analog signal preprocessing for noise reduction and signal acquisition.

risks that the produced TSVs might hit a bonding void leading to increased contact resistance or electrical opens have to be avoided.

A bonded wafer pair with a substrate wafer thickness of $800\ \mu\text{m}$ was investigated. The inspection of those samples was performed through the back-side wafer in order to avoid edge and diffraction artifacts caused by TSV structures in the top wafer. Acoustic inspection was performed using a 175-MHz transducer with a focal length of 8 mm in water at 21°C . The couplant used, which is required for matching acoustic impedances between the acoustical lens and the sample, was degassed and deionized water at 21°C . In order to allow for scanning, the entire wafer was submerged in the couplant during acoustic inspection. For imaging at the highest possible resolution, the acoustic focus was placed at the bond interface by keeping the tip of the acoustic lens $\sim 500\ \mu\text{m}$ above the sample surface. Defects that were of interest in this case study were delaminations of sizes down to $20\ \mu\text{m}$, which may occur at the perimeter of TSV structures. The equipment used herein was a fast scanning acoustic microscope EVOLUTION II (PVA TePla Analytical Systems GmbH). The scan increment was set to $2\ \mu\text{m}$ in order to obtain a maximum in spatial oversampling of the inspected structures resulting in an optimized SNR. Ultrasonic echo signals were digitized at a resolution of 8 bit and a sampling rate of 1 GS/s and stored to the microscope's internal hard drive. For optimizing imaging contrast and resolution, acquired signals were subjected to an off-line signal analysis and the subsequent computation of the exponentially weighted backscatter amplitude integral (BAIⁿ).^{1,2} The algorithm of this signal parameter computation combines the advantages of several mathematical functions with respect to noise suppression and the amplification of

relevant signal energy allowing a reliable detection and imaging of defects way below the resolution limit.

3.1.1 BAIⁿ computation

In the first course, the digitized acoustic signals are rescaled with the average noise level set to <1 . Signal amplitudes are further amplified in a nonlinear manner, resulting in the suppression of signal noise and raising only relevant echo signals by a defined power. The processed signal amplitudes are finally rectified, low-pass filtered, and integrated within a defined time gate.^{2,5}

Figure 2 contains two acoustic micrographs of TSV structures in a bonded wafer pair. TSVs can be seen as bright

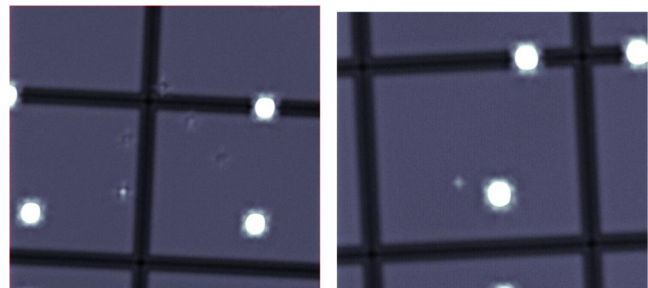


Fig. 2 Scanning acoustic micrographs of a bonded wafer pair through $800\ \mu\text{m}$ of Si recorded at 175 MHz using conventional SAM. Image acquisition was performed through the back-side wafer. The top wafer contained TSV structures with lateral dimensions on the order of $100\ \mu\text{m}$. The images were recorded from two different wafers of the same structure to show voids of various sizes. Extremely small bond voids in the size range of 10 to $20\ \mu\text{m}$ are visible in both images that have been revealed and emphasized using backscatter amplitude integral signal processing of acoustic echo signals.

circular spots. The diameter of the TSVs was on the order of $100\ \mu\text{m}$. The minor white dots that are visible in both images are micro void defects at the bond interface. Micro voids range in size between 10 and $20\ \mu\text{m}$ and can be visualized by acoustic microscopy supplemented with signal processing according to the BAIⁿ algorithm. The images shown in Fig. 2 were obtained from two different wafers of the same structure to show voids of various sizes.

3.2 Acoustic GHz Microscopy Inspection of a Transfer-Bonded 3-D Microbolometer

Acoustic GHz microscopy inspections have been performed on a microbolometer device. For this specific device, the 3-D integration process was based on transfer bonding of a thermistor and a metal reflector onto the readout integrated circuit followed by subsequent removal of the carrier wafer. To control the quality of the transfer step, nondestructive inspection of the bonding interface as well as the device's internal microstructure for irregularities is required. Due to the extremely thin layers and very low total thickness of the microbolometer, conventional SAM in the megahertz range has not been able to allow for internally imaging the device's microstructure. Specifically, the acoustic inspection had to be performed through a $2\text{-}\mu\text{m}$ -thick layer stack consisting of $\text{SiO}_2/\text{Si}/\text{TiAl}/\text{SiO}_2$. Another $0.5\ \mu\text{m}$ below the bonding interface were the TiAl pixel legs. The axial dimensions of the sample's internal structure require a method that

both is extremely sensitive to surface and near-surface structures and allows for penetration into optically opaque materials. Acoustic GHz microscopy allows for both and also provides a lateral resolution sufficient to image the internal structure laterally.^{1,2} It should be emphasized that for the current case study, no destructive or semidestructive preparation of the sample was necessary. The sample was simply taken from one processing step and could have been returned into the manufacturing chain after inspection. However, for the more scientific reason behind this case study, further complementary inspections were performed. For evaluation of the nondestructively detected irregularities by acoustic GHz microscopy, a plasma-FIB (PFIB) processed cross-section has been prepared at the sample. Following the PFIB trenching, scanning electron micrographs have been acquired for visualizing the internal defects with an extremely high resolution. A schematic of the sample is provided in Fig. 3 together with two acoustic micrographs recorded at different defocus. These two images show that the individual pixels of the microbolometer can be visualized through an optically nontransparent layer stack of only a few micrometers thickness using acoustic GHz microscopy. The acoustic micrograph at the lower right even allows for imaging the internal structure at a depth of $\sim 5\ \mu\text{m}$. Acoustic data acquisition at the entire scan area was performed repeatedly at increasing defocus distances (transducer stepwise moved toward the sample). Due to the narrow depth of field of the acoustic lens, the focus is shifted stepwise from the sample

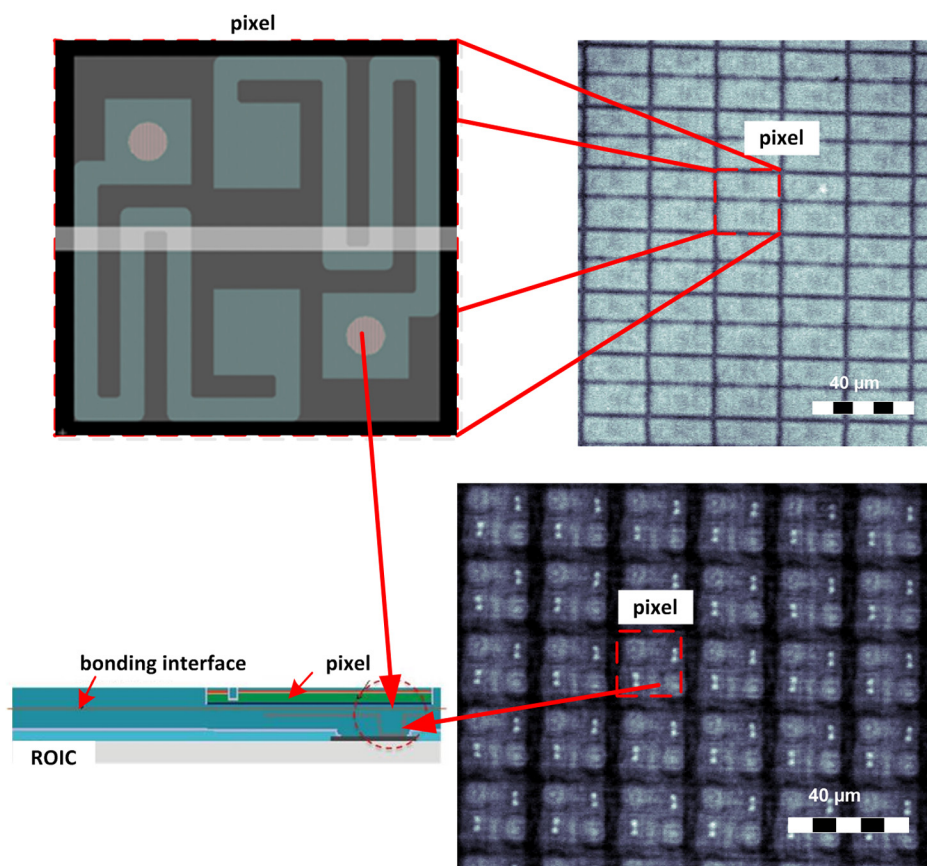


Fig. 3 Schematic of microbolometer investigated by GHz-SAM. The pixel structure is displayed in the images to the left. An acoustic GHz-micrograph at two different defocus positions is shown in the images to the right.

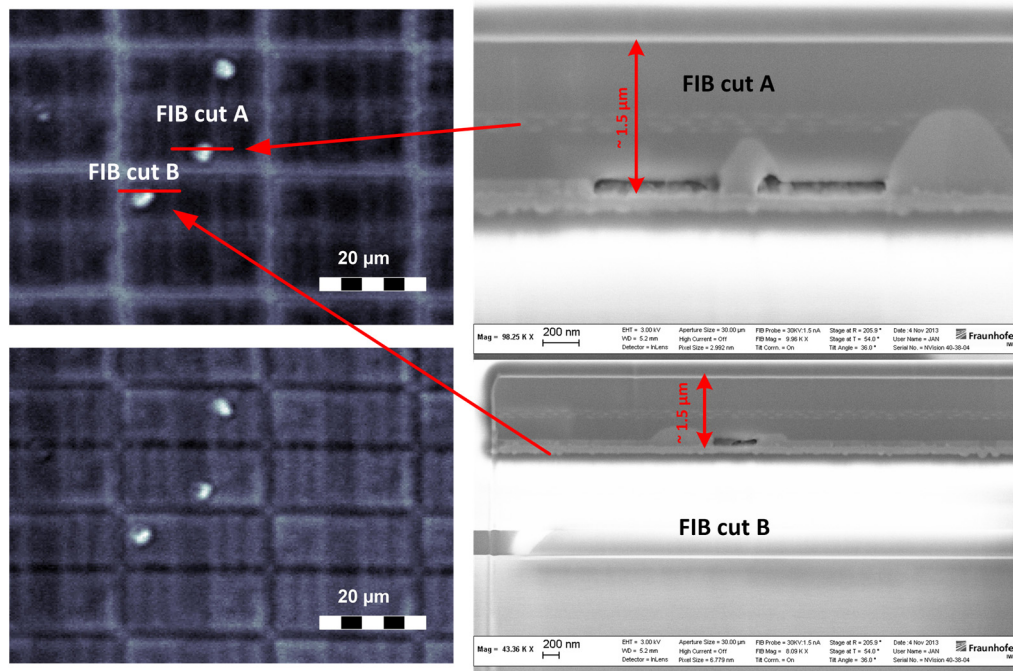


Fig. 4 Results case study II—GHz-SAM inspection of a microbolometer. Left: acoustic GHz-micrographs at different defocus. Gaseous inclusions beneath the sample surface can be seen (bright spots). Right: SE-micrographs of plasma-FIB (PFIB)-prepared cross-sections along red marks in acoustic images (upper left). Voids can be seen at $\sim 2 \mu\text{m}$ beneath sample surface.

surface into the sample and reaches the bond interface during the defocus sequence. Figure 4 contains two acoustic micrographs recorded at 1.12 GHz on the lefthand side. The red markers shown in the upper GHz-SAM image indicated the locations where cross-sectioning was performed using PFIB technology. On the righthand side in Fig. 4, two scanning electron micrographs of the PFIB-prepared cross-sections are shown. Both cross-sections clearly verify the voids that have been indicated using scanning acoustic GHz microscopy. According to the sample manufacturer, these voids are located $\sim 1.5 \mu\text{m}$ beneath the sample surface. The void shown in “cut A” shows a division in its horizontal center. The reason that this pillar is not visible in the acoustic micrograph is that its lateral diameter is $< 100 \text{ nm}$ and, thus, below the resolution limit of the acoustical equipment at this frequency. It should also be noted that the voids may appear larger in the SAM image, which is caused by beam spreading that occurs to the acoustic intensity distribution when the sound waves enter the solid material of the sample. The void shown in the lower-right scanning electron micrograph shows a diameter of $\sim 400 \text{ nm}$ according to its scale bar. This can be explained with the PFIB-prepared cross-section being not localized at the void center and thus cutting it at the outer rim.

3.3 Acoustic GHz Microscopy Inspection on Through Silicon Via Structures

Samples investigated in this case study were copper-filled TSV-technology demonstrators with an aspect ratio of 1:8. This work aimed at the inspection of the TSV fillings and the detection of voids. The equipment and scan procedures applied for acoustic GHz microscopy inspection have been similar to the setup described in the case study above.

The acoustic frequency was 1.12 GHz using an acoustic lens with a focal length of $80 \mu\text{m}$ and an aperture opening angle of 100 deg . The lateral scan field sizes ranged from $\sim 250 \times 250 \mu\text{m}$ to $500 \times 500 \mu\text{m}$. Scans were repeated at an increasing defocus in order to place the acoustical focus inside the TSVs. Even though the theoretical penetration depth does not cover the entire depth of the TSVs, mode conversion of the incident longitudinal wave is expected to occur, allowing the detection of voids inside the TSVs up to a certain depth. The samples inspected here contained a variation of smaller and larger voids as confirmed by PFIB cross-sectioning and scanning electron microscopy (SEM) imaging. Voids that have been found by acoustic GHz microscopy were voids at the upper edge of the filling as well as at

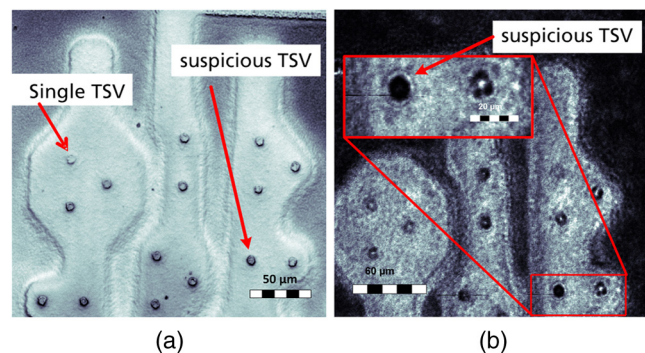


Fig. 5 Acoustic micrographs of TSV structure recorded at 1 GHz acoustic frequency. (a) Image recorded with focus of the acoustic lens at the sample surface. (b) Image recorded with the acoustic lens defocused toward the sample surface. One of the TSVs shows a different acoustic behavior by a notably higher signal intensity.

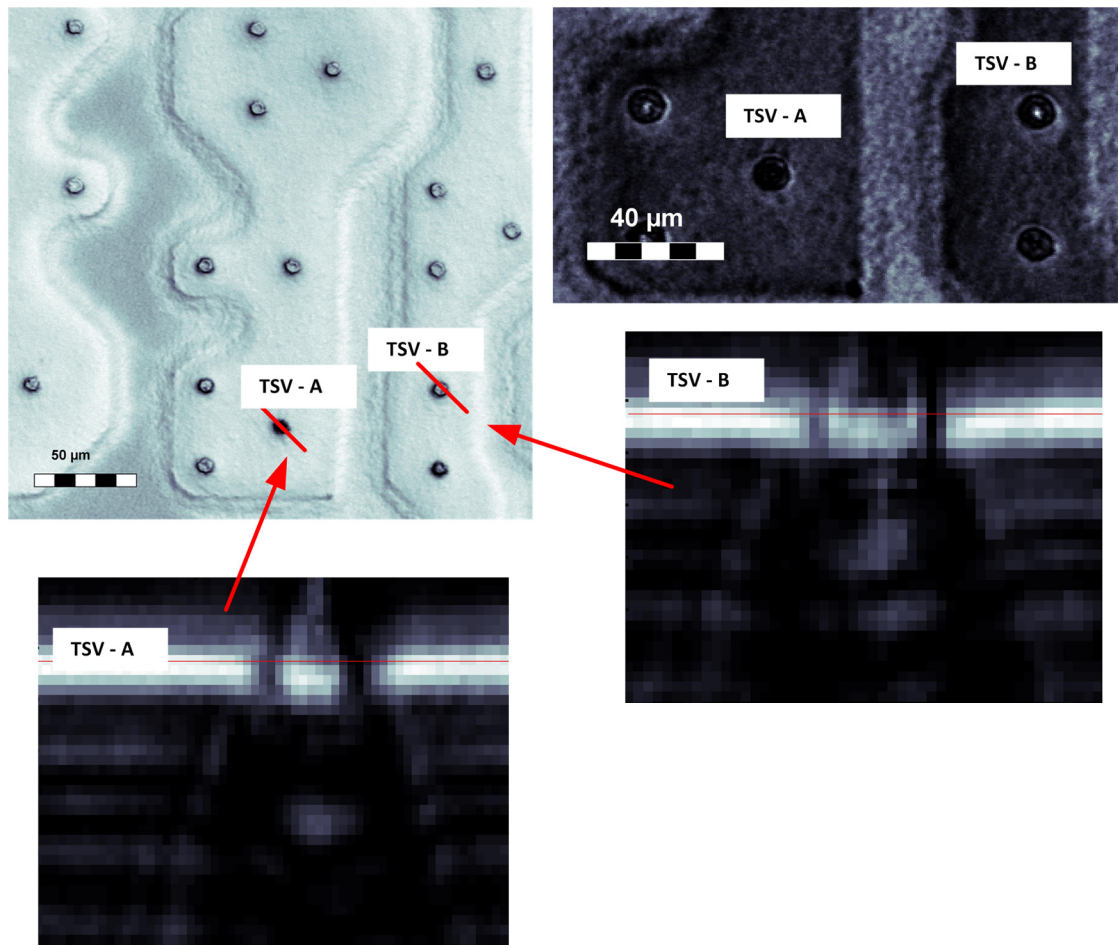


Fig. 6 GHz-SAM inspection of TSV fillings. Upper-left image shows a 500- μm overview of the inspection area. The TSVs named TSV-A and TSV-B are enlarged in the upper-right acoustic GHz-micrograph. At a certain defocus, a bright spot can be seen in TSV-B, while TSV-A does not show that feature. The graphs below show acoustic defocus sequences along the red markers in the overview image in the upper left. Differences in the defocus signature can be observed between TSV-A and TSV-B.

a depth of ~ 8 to $10 \mu\text{m}$. When defocusing the acoustic lens, a differently varying contrast can be noted in the defocused acoustic micrographs shown in Figs. 5, 6, and 7. This difference is not present in images recorded with the sample surface near the focus of the acoustic lens. TSVs showing a contrast variation differing from the majority of the TSVs inspected here are assumed to be suspicious, which requires evidence obtained by physical cross-sectioning and SEM imaging. In the lefthand side image in Fig. 5, a suspicious and a nonsuspicious TSV is marked by a red arrow. Physical cross-sectioning by PFIB and SEM imaging, as presented in Figs. 7 and 8, has revealed voids that correlate to features in the GHz SAM images deviating from the majority of the remaining TSVs. The individual micrographs recorded at decreasing distances between the acoustical lens and the sample surface represent the differently varying features of the $V(z)$ curves, as the method acquires the $V(z)$ curve at each individual scan point of the entire lateral scan area. A differently varying contrast between the individual TSVs is caused by differences in these $V(z)$ curves of the underlying structure. Since the $V(z)$ curve is a material/structure-specific signature,³ features differing between the TSVs are caused by physical differences inside the TSVs (or at their surface). However, since the penetration depth of the

large lens apertures and high frequencies applied here do not allow for inspecting the TSVs over their full depth by only considering the compressional or the Rayleigh wave, it is assumed that further wave modes are excited when either one or both of these modes interact with the structure of a TSV. The theoretical penetration depth using the setup employed here varies with the material inspected and is ~ 1.7 to 2 times the wavelength of the Rayleigh wave here, as described by Atalar.⁶ This corresponds to a penetration depth inside the Si of $8.5 \mu\text{m}$. Even though proof is still required, the authors assume that the excitation of an interface wave propagating vertically in the interface between the TSV and the Si-surrounding, excited by either the incident compressional wave or the Rayleigh wave or both, is not unlikely. It is further assumed that this wave mode propagating in the interface between the TSV and the Si likely leaks energy into the TSV where it will be impacted by its filling condition and should thus be sensitive for detecting voids. Figure 7 contains a zoomed-in section of a GHz SAM micrograph at extreme defocus in the lower-left image. Fringes visible around the individual TSVs can be noted clearly. These fringes have been observed differing between voided and nonvoided TSVs with voids occurring in greater depth ($>8.5 \mu\text{m}$) in work that has not been published so far.

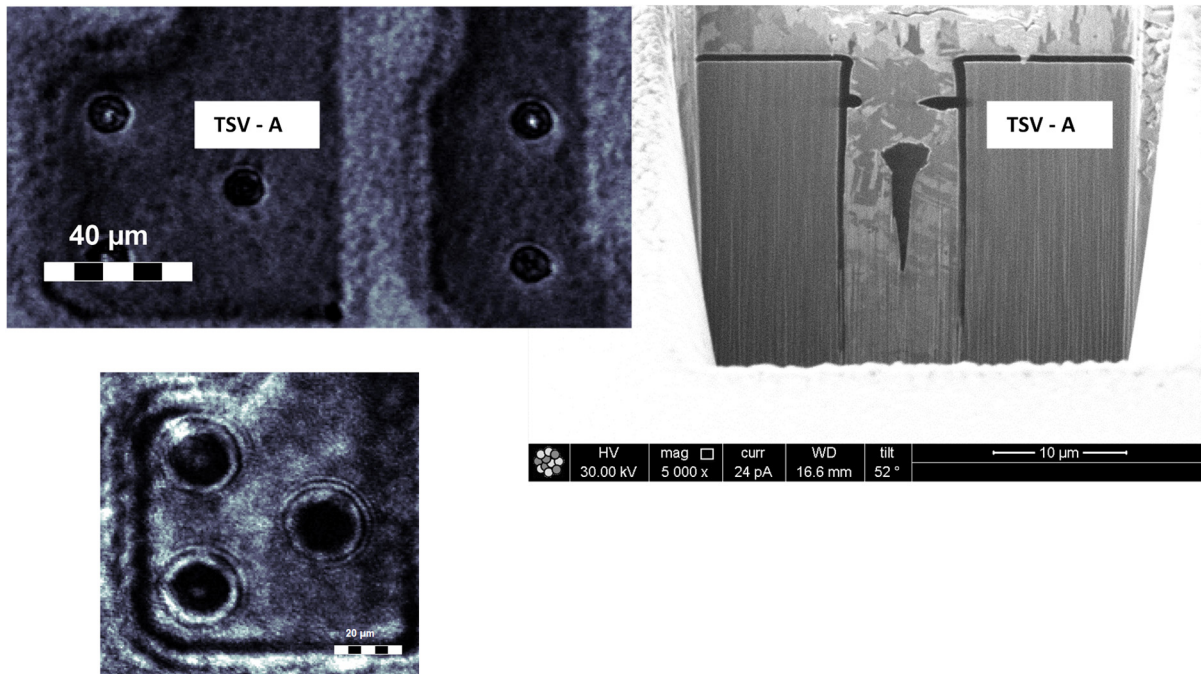


Fig. 7 Verification of acoustic GHz microscopy by PFIB—preparation and SEM imaging. The scanning electron micrograph in the upper-right image shows the physical cross-section through TSV-A. Two smaller and one large void can be identified. No such void has been detected in TSV-B. The lower image shows the section of a GHz-SAM image containing TSV-A at the right. The fringes around TSV-A appear at a different pattern and periodicity when compared to the two other TSVs. This is likely caused by interference between the compressional wave from the surface and potential interface waves propagating in the cylindrical rim of the TSV. Further investigation is required for proof.

As these fringes are definitely caused by an interference of the compressional and/or Rayleigh and likely a further wave component, the investigation of the relationship of this phenomenon and the condition of the TSV filling will be content of future work.

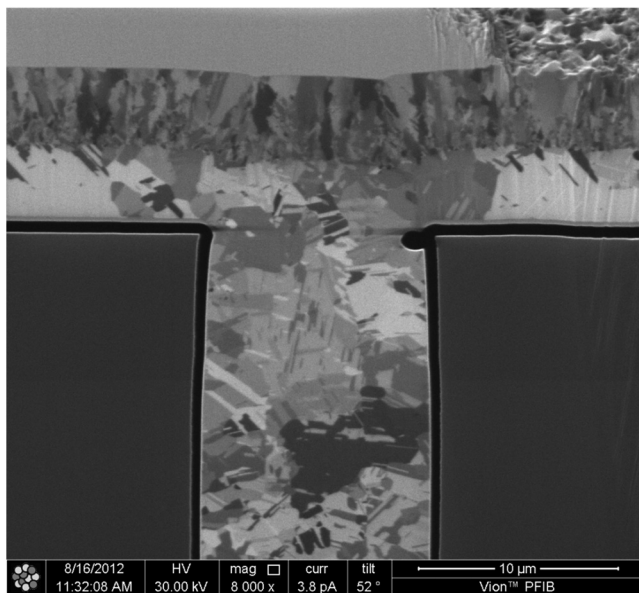


Fig. 8 Scanning electron micrograph of physical cross-section of the TSV showing a high intensity in the acoustic signal in previous figure. A defect at the upper right corner in the TSV filling can be noticed that has been detected acoustically using the GHz-SAM.

4 Outlook

Recent ongoing research studies indicate that GHz SAM might not only be capable of localizing voids in TSV close to the surface as shown in the previous chapter. For Cu-filled TSV with 5- μm diameter and 50- μm depth, first results published in Ref. 7 showed close comparison between GHz SAM defect signals and FIB cross-section validation even if the voids had a depth of $\sim 20 \mu\text{m}$. However, further research is needed to completely employ the full potential of GHz SAM for quality control and defect analysis of TSV. Typically, the penetration depth of ultrasonic waves at high frequencies of 1 GHz is limited to one or two wavelengths due to the narrow depth of field. Insofar, it is necessary to understand which effects contribute to enabling GHz SAM to detect deep voids and to learn more about the applicability, reliability, and limitations of the approach. However, it becomes already clear that high-frequency SAM can provide a beneficial nondestructive technique to control the TSV quality and defect situation.

5 Discussion and Conclusions

In the current paper, the applicability and relevance of acoustic microscopy has been investigated with the focus on emerging technologies for 3-D integration in microelectronics. It has been shown that conventional SAM inspection, even though very helpful, has certain limitations when it comes to microstructures with lateral dimensions $< 15 \mu\text{m}$. Due to acoustic frequency, pulse length, and focusing restrictions, a new concept of acoustic microscopy is required in order to offer the unique benefits provided by acoustic

metrology techniques to technologies in the field of 3-D integration.

It has been shown here that microscopic defects can be detected on full wafer scale using SAM at ~200 MHz acoustic frequency and TSV structures on the order of 100 μm . However, the inspection of TSV fillings or extremely thin films at the wafer bond interface requires much higher spatial resolutions connected with an adjusted SAM concept, operating in GHz frequency band. Acoustic attenuation increases exponentially with frequency and propagation length, challenging acoustic inspection at those extremely high frequencies. Therefore, an adapted transducer and acoustic microscope concept has been necessary for overcoming those issues. The acoustic GHz microscope proved its usefulness in applications of failure analysis and defect assessment in microelectronics.

Acknowledgments

The authors gratefully acknowledge collaboration with Fraunhofer IZM-ASSID as manufacturer of the through silicon via samples and financial support provided from the German "Bundesministerium für Bildung und Forschung

(BMBF)" under contract 13N10972 and the ENIAC Joint Undertaking within the European project ESIP.

References

1. S. Brand et al., "Extending acoustic microscopy for comprehensive failure analysis applications," *J. Mater. Sci.: Mater. Electron.* **22**(10), 1580–1593 (2011).
2. S. Brand et al., "High resolution acoustical imaging of high-density-interconnects for 3D-integration," in *2011 IEEE 61st Electronic Components and Technology Conf.*, Lake Buena Vista, Florida, pp. 37–42 (2011).
3. A. Briggs, *Advances in Acoustic Microscopy*, Plenum Press, New York and London (1995).
4. J. Kraft et al., "3D sensor application with open through silicon via technology," in *2011 Proc. of the 61st Electronics Components Technology Conf.*, Lake Buena Vista, Florida, pp. 560–566 (2011).
5. K. Raum et al., "Channel defect detection in food packages using integrated backscatter ultrasound imaging," *IEEE Trans. Ultrason., Ferroelectr., Freq. Control* **45**(1), 30–40 (1998).
6. A. Atalar, "Penetration depth of the scanning acoustic microscope," *IEEE Trans. Sonics Ultrason.* **32**(2), 164–167 (1985).
7. A. Phommahaxay et al., "High frequency scanning acoustic microscopy applied to 3D integrated process: void detection in through silicon vias," in *Proc. 63rd Electronics Components Technology Conf.*, Las Vegas, Nevada, pp. 227–231 (2013).

Biographies of the authors are not available.